Microfluidic system with integrated electroosmotic pumps, concentration gradient generator and fish cell line (RTgill-W1)—towards water toxicity testing†

Tomasz Glawdel,[a] Caglar Elbuken,[a] Lucy E. J. Lee[b] and Carolyn L. Ren*[a]

Received 10th June 2009, Accepted 18th August 2009
First published as an Advance Article on the web 15th September 2009
DOI: 10.1039/b911412m

This study presents a microfluidic system that incorporates electroosmotic pumps, a concentration gradient generator and a fish cell line (rainbow trout gill) to perform toxicity testing on fish cells seeded in the system. The system consists of three mechanical components: (1) a toxicity testing chip containing a microfluidic gradient generator which creates a linear concentration distribution of toxicant in a cell test chamber, (2) an electroosmotic (EO) pump chip that controls the flow rate and operation of the toxicity chip, and (3) indirect reservoirs that connect the two chips allowing for the toxicant solution to be pumped separately from the electroosmotic pump solution. The flow rate and stability of the EO pumps was measured and tested by monitoring the gradient generator using fluorescence microscopy. Furthermore, a lethality test was performed with this system setup using a rainbow trout gill cell line (RTgill-W1) as the test cells and sodium dodecyl sulfate as a model toxicant. A gradient of sodium dodecyl sulfate, from 0 to 50 μg mL^{-1}, was applied for 1 hr to the attached cells, and the results were quantified using a Live/Dead™ cell assay. This work is a preliminary study on the application of EO pumps in a living cell assay, with the potential to use the pumps in portable water quality testing devices with RTgill-W1 cells as the biosensors.

Introduction

A number of microfluidic platforms with a high degree of functionality[1–3] have been developed to perform a variety of bioassays including single cell analysis,[4,5] cell culture[6–8] and drug discovery.[9,10] Although these devices offer great potential, many are confined to the lab because they require a large infrastructure to operate. This is especially the case with positive displacement pumps such as syringe pumps that use external fluidic connections. In our previous work,[11] we proposed the use of integrated electroosmotic (EO) pumps as an effective alternative for flow control in living cell analysis. Electroosmotic flow (EOF) is not often used with living cells due to concerns that the high electric fields may be lethal to living cells. However, EO pumps overcome this problem by generating a pressure driven flow, from an isolated EOF while still retaining many of the inherent benefits including fast and accurate control of flow rate and direction by manipulating the applied voltage. EO pumps are compact and can be operated from a small power supply or battery pack.[12]

In this work, EO pumps are used in a cell based assay to demonstrate their potential ability for portable applications. The system consists of two glass-slide chips connected by an indirect reservoir system. The toxicity chip contains a microfluidic gradient generator that produces a stable linear gradient in a cell chamber while the EO pumps control the flow rate to the gradient generator. The toxicant studied in this case is sodium dodecyl sulfate (SDS), a common cleansing agent (detergent) and microbicidal agent found in many industrial products that has been identified as a model toxicant for fish toxicity testing.[13] The trout derived gill cell line, RTgill-W1, is used because of its advantages for potential portable water quality testing. RTgill-W1 cells are able to withstand hypo- and hyper-osmotic conditions and grow effectively at room temperature without the need of CO_2 regulation; more importantly, environmental samples can be directly tested without extraction or concentration beforehand.[14]

EO pump performance was characterized by measuring the flow rate output and stability. The maximum flow rate was 2.8 μL min^{-1} under no load when 50 μA of constant current was applied. Good day to day repeatability was achieved through proper maintenance of the pump. The gradient generator performance was characterized by monitoring the concentration of a fluorescent dye in the cell chamber. The ability of the EO pumps to provide effective flow control for a cell based device was examined by performing a lethality test with SDS at a concentration range of 0 to 50 μg mL^{-1} using the RTgill-W1 cells. Results from the chip based assay compared well with a conventional assay performed in microwell plates.

Design

Electroosmotic pump principles

Consider the simplified schematic of the planar microchannel-based EO pump presented in Fig. 1. Please refer to ESI for more

[a]*Department of Mechanical and Mechatronics Engineering, University of Waterloo, 200 University Ave W., Waterloo, ON, Canada N2L 3G1. E-mail: c3ren@mecheng1.uwaterloo.ca; Fax: +1 (519) 888-4567; Tel: +1 (519) 888-4567 x33030*
[b]*Department of Biology, Wilfrid Laurier University, 75 University Ave W., Waterloo, ON, Canada N2L 3C5. E-mail: llee@wlu.ca; Fax: +1 (519) 746-0677; Tel: +1 (519) 884-0710 x2252*

† Electronic supplementary information (ESI) available: Experimental data; fabrication and experimental procedures; and gradient generation movie. See DOI: 10.1039/b911412m

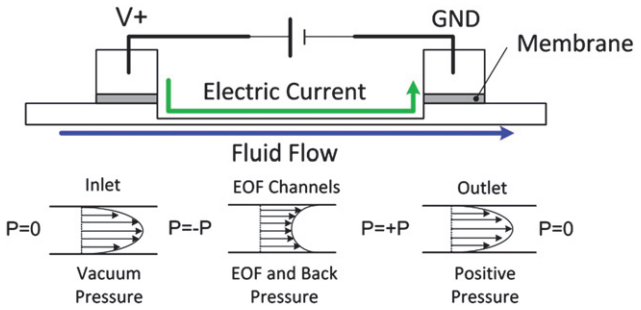

Fig. 1 Schematic of a planar electroosmotic pump describing the electric and flow fields during operation.

details.† EOF is generated in a limited region of the pump by applying an electric field across a network of microchannels. Membranes connect the electrode reservoirs to the fluid flow in the channels, completing the electric circuit but preventing flow into the reservoirs. Consequently, an internal pressure gradient forms to balance mass flow within the pump. Fluid is drawn into the pump by vacuum at the inlet and a positive pressure drives fluid from the outlet. Because of this pressure gradient, the fluid flow in the EOF channels is a combination of EOF and back-pressure flow.

Pump performance is described by the familiar Q–P curve:

$$Q = Q_{\max}\left(1 - \frac{P}{P_{\max}}\right) \quad (1)$$

where $Q_{\max}$ is the maximum flow rate (under no load, *i.e.* the gradient generator is absent from the system) and $P_{\max}$ is the maximum pressure (under infinite load, *i.e.* the gradient generator has an infinitely resistance) at a specified current.

To be able to work with a large range of loads, the EO pumps need to generate a high flow rate which requires a balance where the EOF channels are very shallow in order to maximize the hydrodynamic resistance (R_p) of the pump, but short and wide to minimize the electroosmotic flow resistance (R_{eof}) and the voltage needed to run the pump (IR_e). Please refer to ESI for more details.† In addition, EO pumps work best with solutions that have a low electrical conductivity and high electroosmotic mobility to minimize electrolysis and joule heating while maximizing flow rate and efficiency.

EO pump and toxicity chip design

Fig. 2 shows the microfluidic setup used in this study to perform toxicity experiments with the RTgill-W1 cells. The system is composed of two primary parts: the chip with three EO pumps

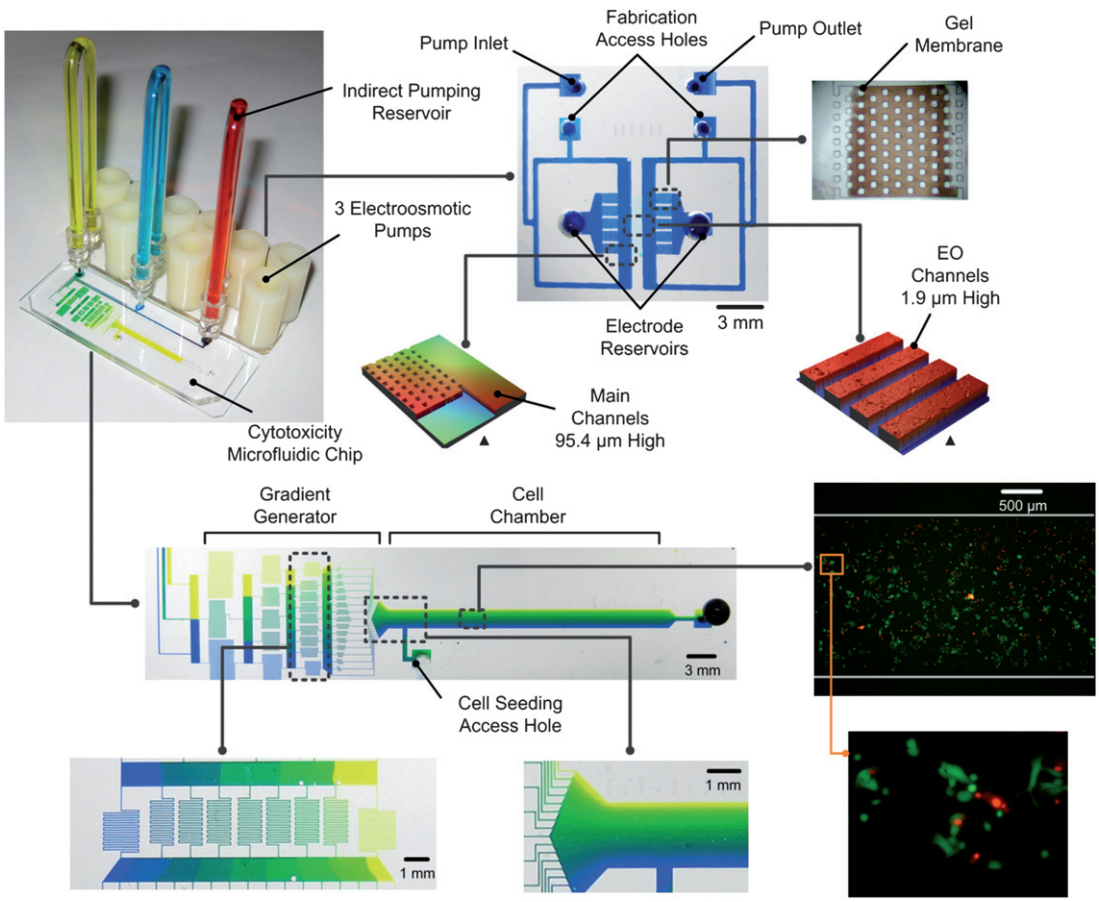

Fig. 2 Three EO pumps fabricated with photopolymerized gel membranes are connected by indirect reservoirs to the toxicity chip which contains a microfluidic gradient generator and test cell chamber. A linear gradient of toxicant is created in the cell chamber and a Live/Dead™ cell assay is used to determine the lethality. The system is built on two separate microscope slides. Pictures are actual images of the chips with colour dyes. ▲indicates 3D profiles of the EO pump design measured with an optical profiler (Wyko NT1100, Veeco).

and the toxicity chip. The EO pumps control fluid flow to the toxicity chip where a gradient generator creates a concentration profile of the toxicant in the cell chamber. Indirect reservoirs connect the two parts and store the fluids used for the toxicity study which is separated from the EO pump fluid by an oil droplet. This scheme allows for a preferential fluid optimized for the EO pumps to be used while allowing for any other solution to be pumped at the same time.

In our previous work,[11] the concept of using EO pumps for living cell analysis was outlined by suggesting a design where the pumps are integrated directly with the cell chambers. The pumps were operated in a vacuum mode where the culture media was drawn over the cells and then through the pump. The attached ESI details the successful culture of RTgill-W1 cells over a period of 10 hr in this configuration.† However, culture media is not ideal for EO pumps because of its high saline content that causes significant electrolysis and joule heating. In addition, with the direct connection of EO pumps and cell chambers, cellular debris would often clog the EO channels limiting the operating lifetime of the pump. Solving these issues drove the development of the more robust design based on the indirect reservoirs.

Indirect reservoir design. The indirect reservoirs are composed of a glass tube (2 mm ID) bent into a U-shape that holds approximately 750 μL of fluid. To prevent leakage, small diameter hydrophobic tubing (0.5 mm ID) was fixed at the outlets to keep the fluid inside the reservoirs *via* surface tension.

EO pump design. The EO pump design used in this work is based on the planar gel salt bridge design of Takamura *et al.*, and is a significant upgrade from our previous work.[11,15] Three independent EO pumps were fabricated at once on one standard microscope slide (1″ × 3″). The new generation design contains 70 parallel EOF channels that are approximately 2 μm (H) and 50 μm (W). Fabrication access ports have been added which allow for solutions to be flushed through the pump without passing them through the EOF channels. This prevents clogging of EOF channels and allows for bubbles to be removed easily. Gel salt bridges fabricated by photopolymerization serve as membranes in the EO pumps to prevent or significantly delay electrolysis effects.

Electrolysis is one of the major issues that restricts EO pump performance and stability. Electrolysis generates H^+ ions at the anode, and OH^- ions at the cathode which alters the local pH and conductivity of the solution. At the anode the pH decreases as does the conductivity (due to a shift in the dissociation equilibrium for a weak buffer), while the opposite occurs at the cathode.[16–18] This causes unstable EOF because the electroosmotic mobility is highly sensitive to the ionic strength and pH of the solution. In addition, electrolysis decomposes water, generating bubbles (H_2 and O_2 gas) at the electrodes which can interrupt the electric connection.

Several precautions were used to provide stable and reliable performance with the EO pumps. First, the gel salt bridges help compartmentalize the electrolysis reaction extending the time it takes for the by-products to reach the fluid flow by diffusion. Secondly, large electrode reservoirs (1 mL) filled with a buffer solution (5 mM Sodium Borate) are used to further absorb the pH change. Thirdly, the pump is operated in a constant current mode rather than constant voltage mode. Changes in the electric circuit due to conductivity changes cause the electric field and therefore flow rate to fluctuate during long term pump operation. Constant current increases stability and pump to pump repeatability and compensates for changes in the pumping environment by always applying a consistent electric field across the EOF channels.[19]

Toxicity chip design. The toxicity chip is composed of a microfluidic gradient generator that leads to a single cell chamber. Microfluidic gradient generators are effective tools for performing bioassays[20,21] as they produce stable, reliable and repeatable gradients of soluble factors.[22] This work uses the compact and efficient design of Campbell and Groisman to create a linear concentration profile.[23] Although a linear gradient was used in this work, any monotonically increasing function can be created through the proper design of the mixing channels using a two-inlet gradient generator.

Because microfluidic gradient generators rely on diffusive mixing, the design must consider the diffusion characteristics of the molecules involved. Using the design equations provided by the authors, the gradient generator was designed to work over a wide range of diffusion coefficients. The limit was set to a diffusion coefficient of $D = 1 \times 10^{-6}$ cm^2 s^{-1} and an output flow rate of 2 μL min^{-1}. The diffusion coefficient of SDS[24] is approximately $D = 7.88 \times 10^{-6}$ cm^2 s^{-1} which allows for the gradient generator to work up to a maximum flow rate of 16 μL min^{-1}. The generator contains four mixing stages that produce 17 stepwise concentrations at the outlet. As the outlet streams merge together, cross stream diffusion causes the stepwise profile to blend together forming the smooth linear gradient profile. Diffusion also causes the gradient to eventually level off downstream in the cell chamber so that there is a working range over which the profile remains constant. For this reason, the chamber was designed to be fairly long in order to accommodate the different molecular characteristics of toxicants that may be studied.

An access port was added to the side of the chamber in order to load the cells so that they do not enter the gradient generator. Dimensions of the cell chamber are 2 mm (W) by 89.7 μm (H), and the serpentine channels in the gradient generator are 50 μm (W). Under the flow rates used in this experiment (max 4 μL min^{-1}), the shear stress on the cells is estimated to be 0.2 dyn cm^{-2}, which is low enough to assume minimal influence on the cells.[8]

Experimental

Materials, fabrication, cell culture and toxicity testing

Refer to ESI for detailed information.†

Electroosmotic pump characterization

Fig. 3 shows the fluidic network used to characterize the performance of the EO pumps. The EO pumps were connected in series with a 15 psi pressure sensor (PX-40, Honeywell) and 40 μL min^{-1} nano-flow sensor (SLG1430-4870, Sensirion). Further downstream, the two sensors were connected different pump loads by a manifold. Each load was controlled by an

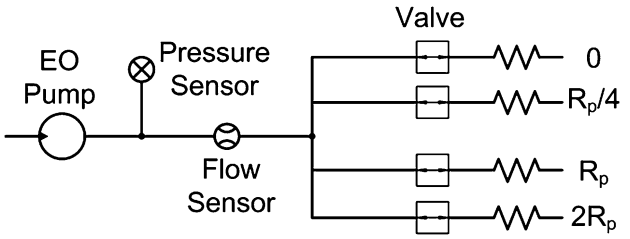

Fig. 3 Schematic of the EO pump testing system consisting of pressure sensor, flow sensor and test loads.

independent valve. The loads were fabricated from small capillary tubing of varying inner diameter and length. Load values were chosen to be approximately 0, ¼, 1, 2 of the pump's hydraulic resistance (R_p). The loads were connected individually and in parallel to represent 33, 50, 60, 80 and 100% of the maximum flow rate (Eqn. (1)). All network components were connected by nano-fittings (Upchurch Scientific) using 0.5 mm ID PEEK tubing resulting in negligible pressure losses and minimal fluidic capacitance in the system. The entire network was fixed onto an optical board.

The protocol for measuring the Q–P curves for the EO pumps is as follows. To remove air bubbles in the fluidic network, the system was flushed using a syringe pump for 30 min. During this time, the EO pumps were placed in a custom chip holder with an electrical circuit connecting to a high voltage sequencer (HVS448, Labsmith). Platinum electrodes were placed in the electrode reservoirs of the three EO pumps. The storage sodium borate solution was then replaced with fresh solution and the pumps were primed at 50 μA for 30 min under no load. The pH (Ag/AgCl, VWR) and electrical conductivity (MI-915, Microelectrodes) of the working fluid was measured beforehand with a pH meter (5 Star Orion, Thermo Electron).

After priming, a single EO pump was tested at a specific constant current by applying the loads sequentially from smallest to largest. At each step the system was allowed to reach a steady state for 5 min, after which measurements were taken and averaged for the next 2 min. This process was repeated three times sweeping through the loads and took approximately 60 min to complete. The same procedure was then repeated for the other pumps. Measurements of the voltage, current, pressure and flow rate were sampled at 10 Hz using a DAQ card (NI-PCI-6221, National Instruments) and an in-house Labview program.

Gradient generator characterization

The EO pump and toxicity chip were mounted on an inverted fluorescence microscope (GX-71, Olympus) with a CCD camera (CoolSNAP ES, Photometrics) and 100 W mercury arc lamp for illumination. Electroosmotic pumps were first tested to determine the Q–P curve for each pump. Indirect reservoirs were connected to two EO pumps, one filled with 100 μM fluorescein dye in pH = 7.5 phosphate buffer and the other with just phosphate buffer. For the gradient generator to work properly the flow rate from both pumps must be the same. Using the Q–P calibration curves already obtained for each pump, the applied currents were set accordingly, given that the pressure load of the cytoxicity chip had already been measured (approximately ¼R_p).

The gradient generator was characterized by relating the flourescence light intensity to the concentration of dye. Images were taken at the entrance to the cell chamber in the toxicity chip. Before evaluating the concentration profile the images were pre-processed (Image Pro Plus) by subtracting the background intensity, and normalizing to a baseline image obtained when the network was flooded with only the fluorescein solution. Normalization compensates for non-uniformity in the illumination and detection sensitivity of the CCD camera. The gradient profiles were then taken and averaged from images over a 5 min period within the experiment.

Results and discussion

EO pump performance

EO pump performance depends strongly on parameters which influence the electroosmotic mobility. These include the pH, ionic strength and composition of the working fluid as well as the surface properties of the channel walls.[25,26] Minimizing changes to these factors is essential in order to achieve stable and repeatable performance. For this reason, a rigorous fabrication protocol was followed. PDMS molds were cured for long periods of time (48 hr, 95 °C) to reduce the amount of left over low molecular weight monomers which are considered the primary cause of electroosmotic mobility decay after plasma treatment.[27,28] After plasma bonding, the EO pumps were filled with fluid and left for two days to let the electroosmotic mobility stabilize.

A number of solutions were tested with the EO pumps in order to optimize performance (1, 5, 10 mM sodium borate). From these tests the best candidate was 5 mM sodium borate (pH = 9.23, $\sigma = 400$ μS cm^{-1}). The high pH and low ionic strength of 5 mM sodium borate results in a large electroosmotic mobility of 5.42×10^{-8} m^2 V^{-1} s^{-1} (measured using the Y-channel current monitoring method[29]). As well, the solution worked within the practical limits of the experimental equipment in terms of generating a measureable current draw for the flow rates needed in this study. To ensure repeatable results, working fluids were tightly regulated by measuring the pH and electrical conductivity before every experiment.

The Q–P curve of each pump that was fabricated during the experiments was measured. Fig. 4A shows the typical Q–P curve obtained for one pump where an external load was added to obtain the generated pressure and flow rate. The curves follow the expected relationship as outlined in Eqn. (1). Pumping flow rate is highly dependent on the geometry of the EO channels ($R_p \propto h^{-3}$). Since fabrication imperfections exist between pumps, each pump has a similar but unique Q–P curve as shown in Fig. 4B. Therefore, the Q–P curve must be measured for all newly fabricated pumps.

Generally pump performance was seen to decrease slightly overtime due to gradual clogging of the EO channels with particles (even though solutions were filtered).The maximum operating time for the pumps was approximately 2.5 hr before electrolysis effects were seen. If the electrolysis limit was exceeded, then the applied voltage increased rapidly due to the drop in conductivity at the anode reservoir. Replacing the solutions did not alleviate the problem as it appears that the resistance of the

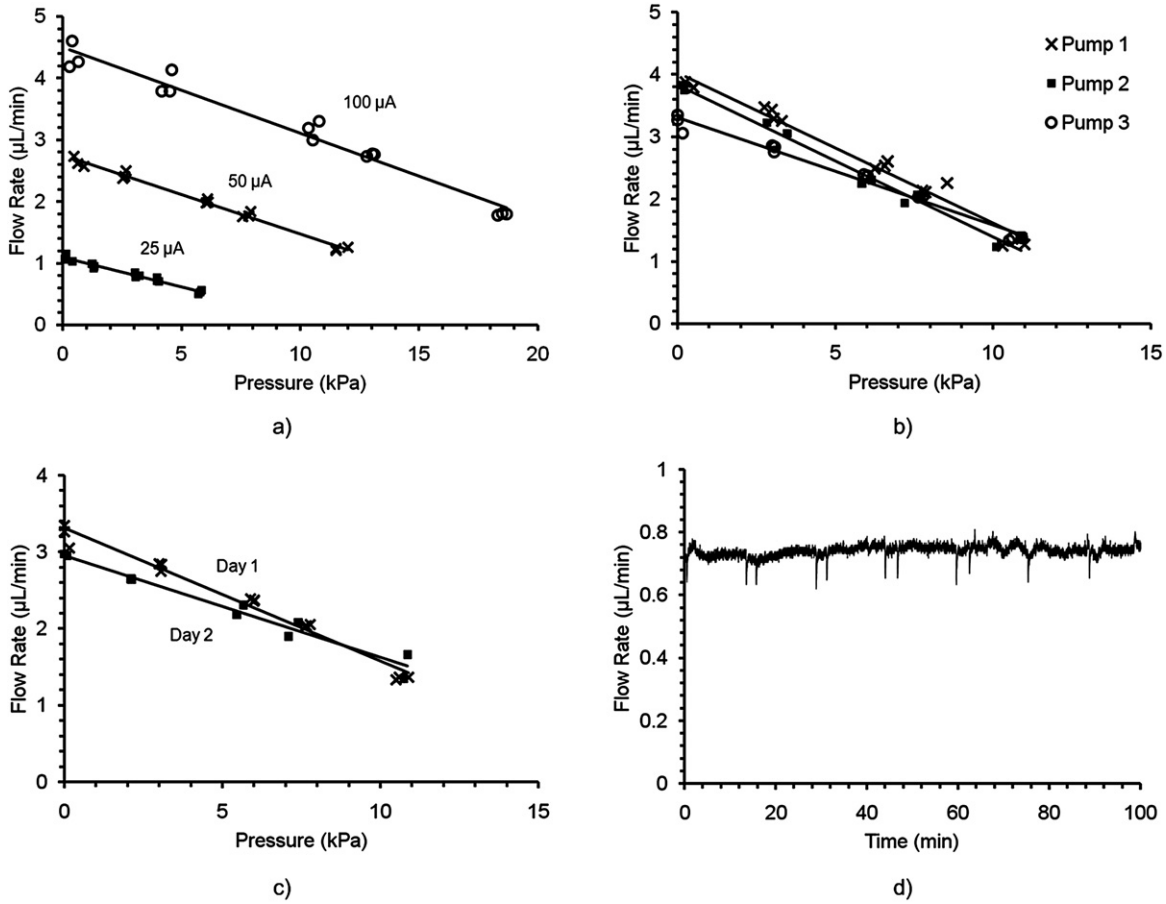

Fig. 4 EO pump characterization curves obtained using the test apparatus (Fig. 3) (a) Q–P curves of an EO pump tested at different applied currents. Pump operation follows the characteristic linear response as outlined in Eqn. (1). (b) Q–P curves for three EO pumps fabricated on the same chip measured on the same day. (c) Q–P curves of an EO pump measured on consecutive days where the electrolysis limit was not exceeded. (d) Flow rate output of an EO pump operating under ½ pump load and constant current mode (50 μA) for 1.5 hr.

gels permanently changes. However, if the solutions were replaced prior to the limit, then the EO pumps could be used several times over the course of a few days. Fig. 4C shows that the day to day repeatability of the EO pumps is fairly consistent. For the gradient generator to work properly the inlet flows must remain constant during the experiment. As seen in Fig. 4D, the EO pumps are able to maintain a steady output for an extended period of time in constant current mode (>1.5 hr). The current and voltage over this period of time is also constant at 50 μA and 220 V (refer to ESI†). The stability can be further improved by integrating flow sensors into the pumps to provide feedback control.[30]

Gradient generation

Prior to the experiments with cells, the performance of the toxicity chip and EO pumps was quantified in terms of the linearity of the gradient generator and its stability. Fluorescein dye was used to quantify mixing using fluorescence microscopy. Two EO pumps were connected to the cytoxicity chip with indirect reservoirs, while the third inlet was plugged. The dye solution was placed in one of the indirect reservoirs and not in the other. The diffusion coefficient of fluorescein is $D = 5 \times 10^{-6}$ cm^2 s^{-1}, which is lower than SDS, and therefore this evaluation represents a worst case scenario in terms of laminar mixing.[23]

The EO pumps were operated at 2 μL min^{-1} for a period of 1 hr. To verify that the gradient generator was working properly, fluorescence images were taken at various stages within the generator as shown in Fig. 5A. Since the design greatly exceeds the requirements for the diffusion of SDS, mixing is completed in only a fraction of the mixing channel length at the flow rates used in this study.

The fluorescein concentration profile was evaluated at the entrance of the cell chamber, after the stepwise concentration had blended together. Fig. 5B shows the normalized fluorescence intensity image and Fig. 5C the profile along the highlighted section. The results match well with the desired linear distribution across the width of the cell chamber. The linear profile deviates a little near the walls of the chamber where small plateaus can be seen. However, these deviations are unavoidable because they are inherent in the design of the gradient generator[23] and are assumed to negligibly influence the toxicity results due to their minute size. The variation in concentration downstream of the entrance was minimal (~2%) over a distance of 2 cm and therefore, cells are exposed to the same concentration of toxicant along the length of the chamber.

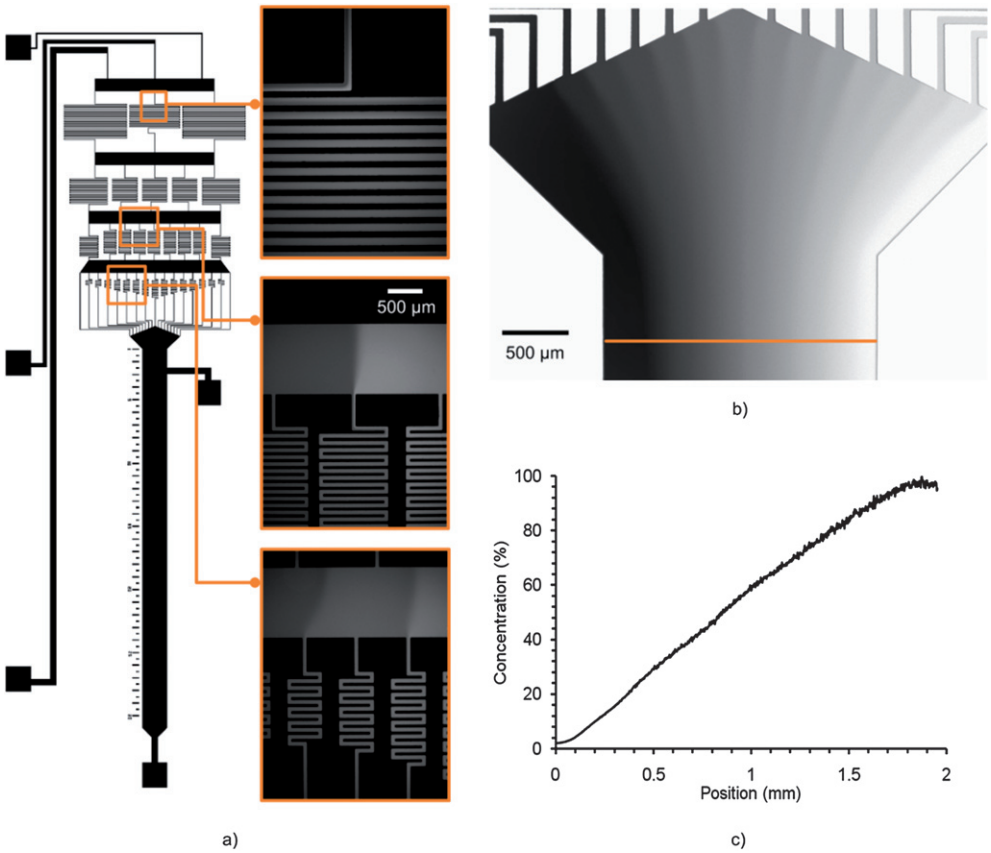

Fig. 5 Evaluation of the concentration gradient generator with the EO pumps using fluorescein dye. (a) Selected fluorescence micrographs showing mixing at different stages in the gradient generator design. (b) Normalized fluorescence micrograph at the outlet of the chamber with a line highlighting the location that the concentration profile is measured. (c) Subsequent plot of the concentration of fluorescein dye based on intensity across the cell chamber, 100% corresponds to the inlet solution containing 100 μM of fluorescein dye. The plot is linear over the width of the chamber except near the walls where small plateaus can be seen.

A video of the EO pumps and toxicity chip operating in a dynamic state has also been provided (refer to ESI†). In this case the EO pumps are programmed to switch between applying a gradient in the cell chamber for 15 min, followed by applying no toxicant gradient for another 15 min. The process is repeated for a period of 2 hr. This represents a potential assay where periodic exposure followed by recovery time could be investigated.

For the gradient generator to work properly, the two inlet flow rates must be balanced, since any deviation will cause the concentration profile to change. If the flow rates are unequal then the mixing ratio will not be correct in the first stage which propagates through the later stages. These experiments with the gradient generator demonstrate that EO pumps and indirect reservoir system are able to precisely regulate the fluid flow in a microfluidic device.

SDS RTgill-W1 toxicity results

The gradient generator and EO pumps were used to perform lethality tests with RTgill-W1 cells and the model toxicant SDS. SDS damages cellular membranes and is classified as a narcotic chemical.[13] Cells were seeded into the cell chamber and a SDS gradient from 0 to 50 μg mL^{-1} was applied for 1 hr. Cell viability was monitored using a Live/Dead™ fluorescence assay kit that was added to the solutions beforehand.

Cells were monitored in an area 5 mm downstream for the cell chamber inlet. The two EO pumps were set to flow rates of 2 μL min^{-1}. The experiment was performed three times on different toxicity chips and with different EO pumps. Fig. 6 shows images collected from one of these experiments. For the quantitative investigation, a rectangular mesh was overlaid on the image. The grid contained 20 rows, each representing 2.5 μg mL^{-1} increments of SDS concentration, over a 3 mm section of the cell chamber. The number of alive cells (green) and dead cells (red) were counted for each row. Fig. 7 demonstrates the process by which the quantitative analysis was performed with the grids. Results were tabulated as the percentage of dead cell in each division.

Fig. 8 summarizes the results for different exposure times. The death rate rises steadily with exposure time under the applied gradient. The LC50 (lethal concentration to kill 50% of organisms) at 15, 30 and 60 min is not detectable, 50 μg mL^{-1}, and 37.5 μg mL^{-1} respectively. For comparison, experiments were performed under similar conditions in standard microwell plates using the fluorometric assay Alamar Blue (refer to ESI for details†). The LC50 for exposure times of 15, 30 and 60 min were 60.64 μg mL^{-1}, 55.95 μg mL^{-1}, and

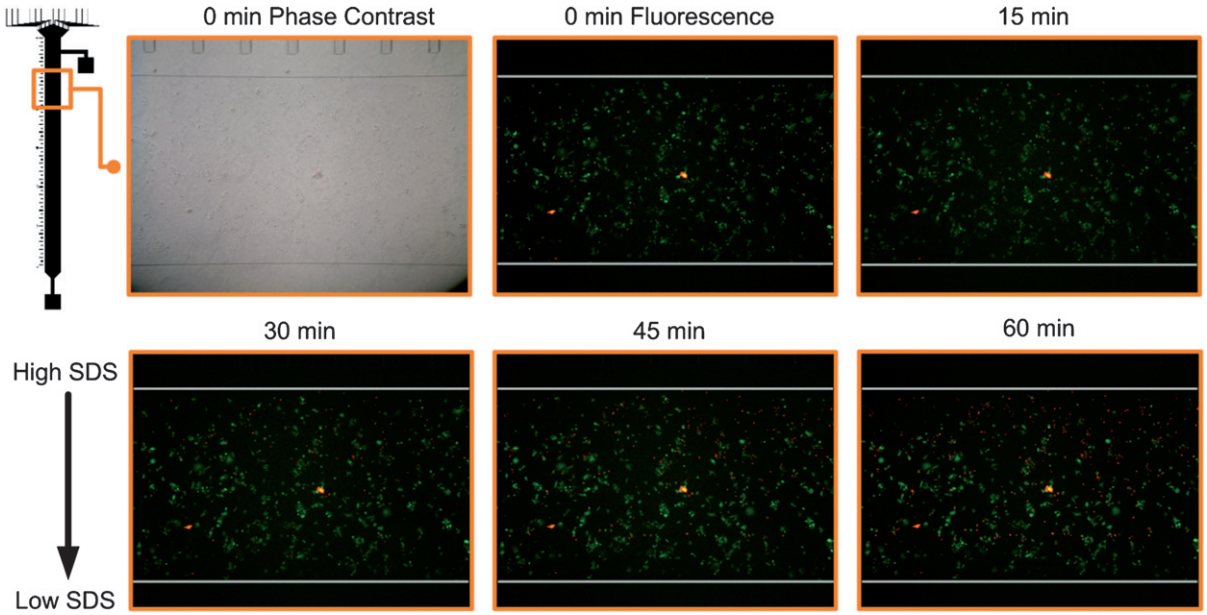

Fig. 6 Results gathered from a toxicity experiment with SDS and RTgill-W1 cells. A gradient from 0–50 μg mL^{-1} SDS in L15ex media was applied for 1 h at a combined flow rate of 4 μL min^{-1}. Sequential fluorescence images showing the Live/Dead™ cell assay at different times in the experiment. Live cells are green and dead cells red. The concentration varies from bottom (low) to the top (high) in the images and covers a 3 mm area in the cell chamber.

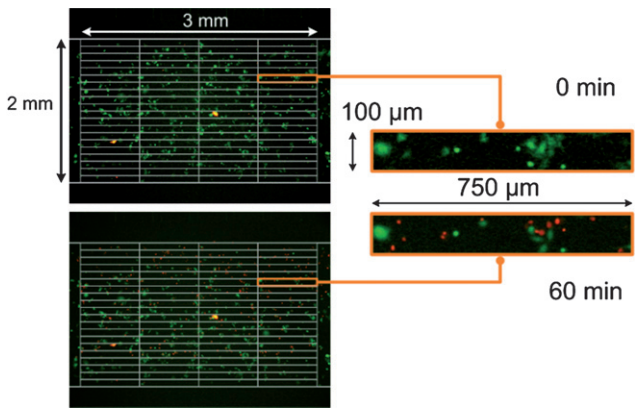

Fig. 7 Cell mortality was tabulated by overlaying a rectangular mesh (20 × 4) over the images and counting the number of alive (green) and dead (red) cells in each division. Insets show the change between the beginning and end of the experiment at one grid location.

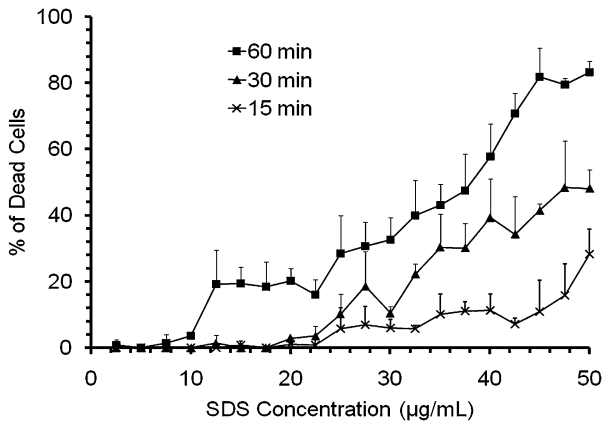

Fig. 8 Quantitative results of the toxicity study in terms of the percent of dead cells at 15, 30 and 60 min with an applied SDS gradient from 0–50 μg mL^{-1}. Results are from three experiments performed with different toxicity chips and EO pumps. Only positive error bars are shown for clarity and represent the standard deviation from all experiments (n = 3).

35.22 μg mL^{-1}. These results agree well with the chip based assay.

Comparing the results with other toxicity data for SDS. The LC50 for human epithelial gingival cells after 24 hr exposure is 75 μg mL^{-1}.[31] Therefore, this assay was far more sensitive than human gingival cells and at a fraction of the time required to evaluate with human cells. Material Safety Data Sheets (MSDS from Sigma) for SDS indicate an LC50 for whole rainbow trout after 96 hr to be 3.6 μg mL^{-1} which appears to be more sensitive, however, this is the value obtained after 96 hr exposure, not after 1 hr as performed here. As our graphic trend indicates, the SDS concentrations needed to obtain a 50% kill decreases with increasing time, thus it is expected that the effective concentration to kill 50% of the cells with longer exposure periods would likely be much less, in agreement with the *in vivo* data.

Conclusions

The goal of this study was to demonstrate the possibility of using electroosmotic pumps for a cell based assay that requires stringent flow control. EO pumps were fabricated on chip with photopolymerized gel salt bridges. An indirect pumping reservoir system was used to separate the test fluid from the EO pumping fluid. As part of this work, the performance of the pumps in terms of repeatability and stability was evaluated by measuring the Q–P curves of the pump and the long term pumping ability.

Using the stable output flow of the flow control system a toxicity test with RTgill-W1 cells and sodium dodecyl sulfate was successfully performed.

The future goal is to incorporate the EO pumps in a portable cell based assay for water quality testing along the same lines as the portable mammalian based device recently published by Curtis *et al.*[32] This will require the development of a small power supply as well as integrated detectors to measure the cell response. We believe that EO pumps combined with RTgill-W1 cells as the biosensor can potentially produce a highly compact Lab-on-a-Chip device for water quality testing.

Acknowledgements

The authors gratefully acknowledge the support from Natural Science and Engineering Research Council of Canada for research grants to Dr. Carolyn Ren and Dr. Lucy Lee and research support to Dr. Caglar Elbuken, Ontario's Early Research Award to Dr. Carolyn Ren and the Canada Graduate Scholarship (CGS) to Tomasz Glawdel.

References

1 A. J. deMello, *Nature*, 2006, **442**, 394–402.
2 G. M. Whitesides, *Nature*, 2006, **442**, 368–373.
3 J. El-Ali, P. K. Sorger and K. F. Jensen, *Nature*, 2006, **442**, 403–411.
4 A. R. Wheeler, W. R. Throndset, R. J. Whelan, A. M. Leach, R. N. Zare, Y. H. Liao, K. Farrell, I. D. Manger and A. Daridon, *Anal. Chem.*, 2003, **75**, 3581–3586.
5 D. Di Carlo, L. Y. Wu and L. P. Lee, *Lab Chip*, 2006, **6**, 1445–1449.
6 I. Meyvantsson and D. J. Beebe, *Annu. Rev. Anal. Chem.*, 2008, **1**, 423–449.
7 A. L. Paguirigan and D. J. Beebe, *Integr. Biol.*, 2009, **1**, 182–195.
8 L. Kim, Y. C. Toh, J. Voldman and H. Yu, *Lab Chip*, 2007, **7**, 681–694.
9 A. Khademhosseini, *Expert Rev. Mol. Diagn.*, 2005, **5**, 843–846.
10 J. Pihl, M. Karlsson and D. T. Chiu, *Drug Discovery Today*, 2005, **10**, 1377–1383.
11 T. Glawdel and C. L. Ren, *Mech. Res. Commun.*, 2009, **36**, 75–81.
12 D. Erickson, D. Sinton and D. Q. Li, *Lab Chip*, 2004, **4**, 87–90.
13 K. Schirmer, K. Tanneberger, N. I. Kramer, D. Volker, S. Scholz, C. Hafner, L. E. J. Lee, N. C. Bols and J. L. M. Hermens, *Aquat. Toxicol.*, 2008, **90**, 128–137.
14 L. E. J. Lee, V. R. Dayeh, K. Schirmer and N. C. Bols, *In Vitro Cell. Dev. Biol.: Anim.*, 2009, **45**, 127–134.
15 Y. Takamura, H. Onoda, H. Inokuchi, S. Adachi, A. Oki and Y. Horiike, *Electrophoresis*, 2003, **24**, 185–192.
16 M. S. Bello, *J. Chromatogr., A*, 1996, **744**, 81–91.
17 D. P. de Jesus, J. G. A. Brito-Neto, E. M. Richter, L. Angnes, I. G. R. Gutz and C. L. do Lago, *Anal. Chem.*, 2005, **77**, 607–614.
18 D. G. Yan, C. Yang and X. Y. Huang, *Microfluid. Nanofluid.*, 2007, **3**, 333–340.
19 A. Brask, J. P. Kutter and H. Bruus, *Lab Chip*, 2005, **5**, 730–738.
20 B. G. Chung, L. A. Flanagan, S. W. Rhee, P. H. Schwartz, A. P. Lee, E. S. Monuki and N. L. Jeon, *Lab Chip*, 2005, **5**, 401–406.
21 J. Y. Park, C. M. Hwang, S. H. Lee and S. H. Lee, *Lab Chip*, 2007, **7**, 1673–1680.
22 T. M. Keenan and A. Folch, *Lab Chip*, 2008, **8**, 34–57.
23 K. Campbell and A. Groisman, *Lab Chip*, 2007, **7**, 264–272.
24 A. C. F. Ribeiro, V. M. M. Lobo, E. F. G. Azevedo, M. G. Miguel and H. D. Burrows, *J. Mol. Liq.*, 2003, **102**, 285–292.
25 B. J. Kirby and E. F. Hasselbrink, *Electrophoresis*, 2004, **25**, 187–202.
26 B. J. Kirby and E. F. Hasselbrink, *Electrophoresis*, 2004, **25**, 203–213.
27 D. T. Eddington, J. P. Puccinelli and D. J. Beebe, *Sens. Actuators, B*, 2006, **114**, 170–172.
28 J. Kim, M. K. Chaudhury, M. J. Owen and T. Orbeck, *J. Colloid Interface Sci.*, 2001, **244**, 200–207.
29 Z. A. Almutairi, T. Glawdel, C. L. Ren and D. A. Johnson, *Microfluid. Nanofluid.*, 2009, **6**, 241–251.
30 K. Seibel, L. Scholer, H. Schafer and M. Bohm, *J. Micromech. Microeng.*, 2008, **18**.
31 H. Babich and J. P. Babich, *Toxicol. Lett.*, 1997, **91**, 189–196.
32 T. M. Curtis, M. W. Widder, L. M. Brennan, S. J. Schwager, W. H. van der Schalie, J. Fey and N. Salazar, *Lab Chip*, 2009, **9**, 2176–2183.

